ADVANCES IN ATMOSPHERIC SCIENCES, VOL. 28, NO. 6, 2011, 1246–1258

Weakening of Interannual Variability in the Summer East Asian Upper-tropospheric Westerly Jet since the Mid-1990s

LU Riyu*[1] (陆日宇), YE Hong[1] (叶 红), and Jong-Ghap JHUN[2]

[1]*State Key Laboratory of Numerical Modeling for Atmospheric Sciences and Geophysical Fluid Dynamics, Institute of Atmospheric Physics, Chinese Academy of Sciences, Beijing* 100029

[2]*School of Earth and Environmental Sciences, Seoul National University, Seoul, Korea*

(Received 10 December 2010; revised 20 February 2011)

ABSTRACT

In this study, we found that the intensity of interannual variability in the summer upper-tropospheric zonal wind has significantly weakened over Northeast Asia and the subtropical western North Pacific (WNP) since the mid-1990s, concurrent with the previously documented decrease of the westerly jet over North China and Northwest China. Corresponding to this weakening of zonal wind variability, the meridional displacement of the East Asian westerly jet (EAJ) manifested as the leading mode of zonal wind variability over the WNP and East Asia (WNP–EA) before the mid-1990s but not afterward. The energetics of the anomalous pattern associated with the meridional displacement of the EAJ suggests that barotropic energy conversion, from basic flow to anomalous patterns, has led to the weakening of the variability in the EAJ meridional displacement and to a change in the leading dominant mode since the mid-1990s. The barotropic energy conversion efficiently maintained the anomalies associated with the variability in the EAJ meridional displacement during 1979–1993 but acted to dampen the anomalies during 1994–2008. A further investigation of the energetics suggests that the difference in the patterns of the circulation anomaly associated with either the first leading mode or the meridional displacement of the EAJ, i.e., a southwest–northeast tilted pattern during 1979–1993 and a zonally oriented pattern during 1994–2008, has contributed greatly to the change in barotropic energy conversion.

Key words: East Asian jet, mid-1990s, interannual variability, energetics

Citation: Lu, R. Y., H. Ye, and J.-G. Jhun, 2011: Weakening of interannual variability in the summer East Asian upper-tropospheric westerly jet since the mid-1990s. *Adv. Atmos. Sci.*, **28**(6), 1246–1258, doi: 10.1007/s00376-011-0222-5.

1. Introduction

The westerly jet over the midlatitude western North Pacific and East Asia (WNP–EA) plays a crucial role in maintaining the subtropical summer rain band, which is well known as Meiyu in China, Changma in Korea, and Baiu in Japan. This westerly jet tilts significantly northward with height. Generally, the upper-tropospheric westerly jet core is located to the north of the subtropical rain band, while the lower-tropospheric jet core is located to the south of the rain band. Additionally, the lower-tropospheric westerly jet, or, more exactly, the southwesterly jet, supplies water vapor to the rain band. Recently, Sampe and Xie (2010) suggested that the westerly jet in the middle troposphere can lead to the subtropical rain band through warm horizontal temperature advection and by steering transient eddies.

On the interannual time scale, the East Asian upper-tropospheric westerly jet (hereafter EAJ in short) is also closely related to summer rainfall along the subtropical rain band over the WNP–EA, although the interannual variability and climatological aspects of the subtropical rainfall may be governed by different mechanisms. For instance, in the summer, when the EAJ is displaced northward, rainfall is suppressed along the subtropical rain band, and when the EAJ is displaced southward, rainfall is enhanced along the subtropical rain band (Lau et al., 2000; Lu, 2004). The meridional displacement of the EAJ is the first lead-

*Corresponding author: LU Riyu, lr@mail.iap.ac.cn

© China National Committee for International Association of Meteorology and Atmospheric Sciences (IAMAS), Institute of Atmospheric Physics (IAP) and Science Press and Springer-Verlag Berlin Heidelberg 2011

ing mode of upper-tropospheric zonal wind variability over the WNP–EA, and the second mode is the intensity change in the EAJ (Lin and Lu, 2005). The meridional displacement of the EAJ can also serve as a bridge linking previous winter ENSO and early summer rainfall in China (Lin and Lu, 2009).

The meridional displacement of the EAJ, which is affected by an eastward-propagating wave train along the Asian jet (Lu et al., 2002; Enomoto et al., 2003), is a manifestation of the meridional teleconnection over the WNP–EA. This meridional teleconnection is characterized by the zonally elongated anomalies of both precipitation and circulation, which appear in alternate signs in the meridional direction from tropical WNP to the mid-high latitudes (e.g., Nitta, 1987; Huang and Sun, 1992; Lau et al., 2000; Wang et al., 2001; Lu, 2004; Hsu and Lin, 2007; Lu and Lin, 2009; Kosaka and Nakamura, 2010). The meridional teleconnection has been previously explained by the northward propagation of Rossby waves triggered by anomalous convection over the tropical WNP (e.g., Kurihara and Tsuyuki, 1987; Nitta, 1987; Huang and Sun, 1992). Recent studies, however, have suggested that the mechanisms for the maintenance of the meridional teleconnection involve many features: midlatitude wave activity (Enomoto et al., 2003; Bueh et al., 2008; Shi et al., 2009; Shi and Lu, 2010), vertically sheared tropical mean zonal flow (Lu, 2004; Lin et al., 2010), circulation–rainfall interaction (Lu and Lin, 2009), and a moist dynamical mode in the zonally asymmetric baroclinic mean flow (Kosaka and Nakamura, 2006, 2010).

Kosaka and Nakamura (2006, 2010) reported that the meridional teleconnection pattern (the Pacific–Japan pattern in their paper) can gain energy from the mean flow over the WNP–EA. The climatological mean flow over the WNP–EA has a unique three-dimensional structure, characterized by the midlatitude westerly jet in the upper troposphere, by the summer monsoonal flow to the west, and by the subtropical anticyclone to the east in the lower troposphere. Therefore, it can be reasonably hypothesized that the meridional teleconnection might be affected by changes in the basic flow.

East Asian summer monsoon, including the aspects of both rainfall and circulation, exhibits a clear variation on the decadal/interdecadal time scale (e.g., Wang, 2001; Zhu and Wang, 2001; Gong and Ho, 2002; Li et al., 2004; Kim et al., 2010), and these low-frequency oscillations may provide different backgrounds for interannual variations by inducing different basic flows in different periods. The possible mechanisms responsible for the variation include the impacts of SST (Huang et al., 1999; Zhu and Yang, 2003; Lu et al., 2006; Li and Bates, 2007; Fu et al., 2009; Gu et al., 2009; Zhou et al., 2009; Yun et al., 2010; Zhu et al., 2010), upper-tropospheric cooling (Yu and Zhou, 2007), Eurasian snow cover (Wu et al., 2009), and North Pacific sea ice (Choi et al., 2009). These studies suggest the existence of many transferring points for the decadal/interdecadal variation in the East Asian summer climate, for instance, around the late 1970s (Huang et al., 1999; Wang, 2001; Gong and Ho, 2002; Yu and Zhou, 2007) and the late 1990s (Yun et al., 2010; Zhu et al., 2010).

In addition to the transferring points for the decadal/interdecadal variation mentioned above, a recent study by Kwon et al. (2007) indicated that the East Asian summer climate experienced a decadal change in the mid-1990s. After the mid-1990s, the upper-tropospheric westerly jet over North China and Northwest China weakened significantly, and precipitation was enhanced in South China. Kwon et al. (2007) suggested that the weakening of the upper-tropospheric westerly jet was induced by the enhanced precipitation over South China, as a barotropic response to the heat forcing of increased precipitation. Kwon et al. (2007) suggested that more landfalling typhoons have resulted in the increase of South China rainfall. On the other hand, Wu et al. (2010) identified a slightly earlier transferring point (1992–1993) of interdecadal change in South China rainfall, and they have suggested that the changes in the Tibetan Plateau snow cover and equatorial Indian SST lead to this interdecadal change in rainfall. Some further previous studies identified significant interdecadal changes in the mid-1990s in the relationship among the East Asian monsoon, WNP monsoon and ENSO on the interannual time scale (Kwon et al., 2005; Yim et al., 2008a, b).

Concerning the background changes associated with the interdecadal changes in the mid-1990s, do the intensity and leading modes of interannual variability change? If so, what is the mechanism responsible for the change? These questions were investigated in this study using National Centers for Environmental Prediction/Department of Energy (NCEP/DOE) Reanalysis 2 data. The arrangement of the text is as follows. We show the change in intensity of EAJ interannual variability around the mid-1990s in section 2, and we show the change in the dominant modes of EAJ variability in section 3. Section 4 is devoted to an analysis of energetics, in an attempt to illustrate the mechanism responsible for the changes in the EAJ interannual variability associated with the background change in the mid-1990s. A summary is provided in section 5.

2. Weakening of the EAJ interannual variability since the mid-1990s

During summer, an upper-tropospheric westerly jet stream with maximum zonal velocity of 20–30 m s^{-1} appears over the Eurasian continent and extends eastwards to the North Pacific (Fig. 1a). Its axis is oriented in a zonal direction along 40°N over the Eurasian continent, and it curves slightly northeastward over the North Pacific. The maximum core appears over Northwest China, with a zonal velocity >30 m s^{-1}. This is a unique feature of EAJ in summer, because in other seasons the EAJ core is located over the WNP (Zhang et al., 2006).

Figure 1b shows the interannual standard deviations of June–July–August (JJA) mean zonal winds at 200 hPa. The relatively greater variability in the zonal winds appears over North China, Korea, Japan, and Northeast Asia. This distribution differs somewhat from previous results. Previous studies have shown two regions of strong zonal wind variability, one extending from central China northeastward into the North Pacific (∼30°–40°N), and the other located over Northeast Asia (∼40°–50°N) (Lu, 2004; Lu and Fu, 2010). Between these two regions is a zonally oriented belt of relatively weaker zonal wind variability. Therefore, in these previous results, the interannual standard deviations of 200-hPa zonal winds manifested in the shape of a saddle. In the results of this study, however, such a belt of weaker variability can hardly be found, and thus the saddle shape disappears. This discrepancy between these results and those of previous results (which are further discussed in the following section) is basically due to the different periods of analysis. The wind data for this study were from the period 1979–2008, but they were from 1979–1998 in Lu (2004) and from 1948–2008 in Lu and Fu (2010).

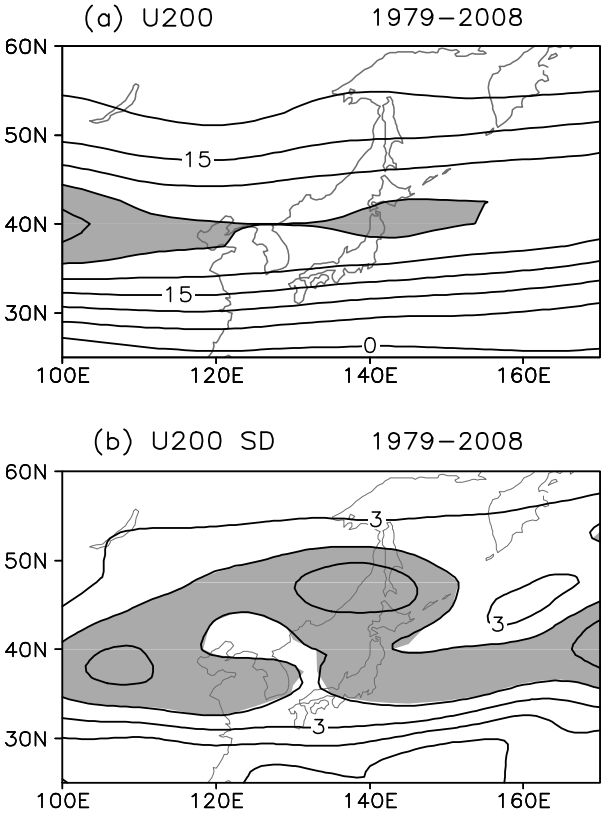

Fig. 1. Climatological JJA-mean 200-hPa zonal wind (a) and standard deviation (b), averaged over 1979–2008. Shading indicates the regions where the values are >25 m s^{-1} and 3.5 m s^{-1}; the contour intervals are 5 m s^{-1} and 0.5 m s^{-1} in (a) and (b), respectively.

The dependency of the spatial structure of zonal wind standard deviations on periods is confirmed by Fig. 2. Following Kwon et al. (2005, 2007), we divided the analysis period into two periods: before and after 1993–1994, i.e., 1979–1993 and 1994–2008, and we compared the features of zonal wind variability during the two periods (Fig. 2). During the period of 1979–1993, stronger interannual variability is located around 35°N and 45°N, respectively, and weaker variability is located in between (around 40°N), resembling a saddle shape (Fig. 2a). During the period of 1994–2008, however, zonal wind variability becomes weaker around 35°N and 45°N, but does not change much around 40°N (Fig. 2b). Therefore, during the latter period, there is no longer a relatively stronger variability around 35°N and 45°N and weaker variability in between, and thus the saddle shape disappears.

Another significant difference between the two periods is the change in magnitude of zonal wind variability. The interannual standard deviations of zonal winds are stronger during the former period and weaker during the latter period, as indicated by the shrinkage of shading areas (values >3.5 m s^{-1}) in Figs. 2a and b. The weakening of interannual variability is statistically significant over the WNP south of Japan and is marginally significant around 45°N (Fig. 2c). These regions of weakened variability overlap with the two averaging areas for the EAJ index, which was defined by Lu (2004) to measure the meridional displacement of the JJA-mean EAJ. Lu (2004) measured the meridional displacement of the EAJ using the difference between the 200-hPa zonal wind anomalies averaged over (30°–40°N, 120°–150°E) and (40°–50°N, 120°–150°E). In this study, we used this EAJ index (EAJI); thus, a positive EAJI indicates a southward displacement of the EAJ, and a negative EAJI indicates a northward displacement of the EAJ.

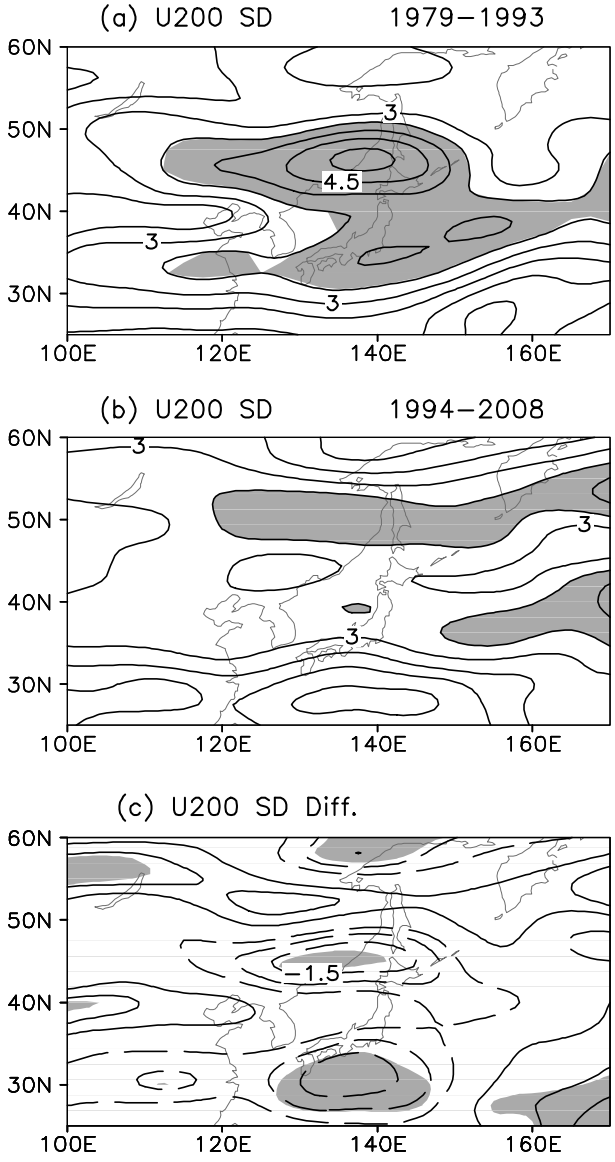

Fig. 2. Standard deviation of 200-hPa zonal wind during (a) 1979–1993 and (b) 1994–2008, and their difference (a minus b, c). The contour interval is 0.5 m s^{-1}. Shading indicates the regions where the values are >3.5 m s^{-1} in (a) and (b), and shading in (c) indicates the difference in the standard deviation at the 95% confidence level according to the F-test.

Therefore, Fig. 2c suggests a weakening of the interannual variability in the EAJI during the latter period. Figure 3 confirms this. The EAJI tends to become weaker, indicated by the line shown in Fig. 3, and particularly, has been much weaker since 1995. One standard deviation during the entire period (1979–2008) is 4.42, and there are six years (1980, 1982, 1984, 1985, 1990 and 1993) in which the EAJI anomaly exceeds this value during the former period,

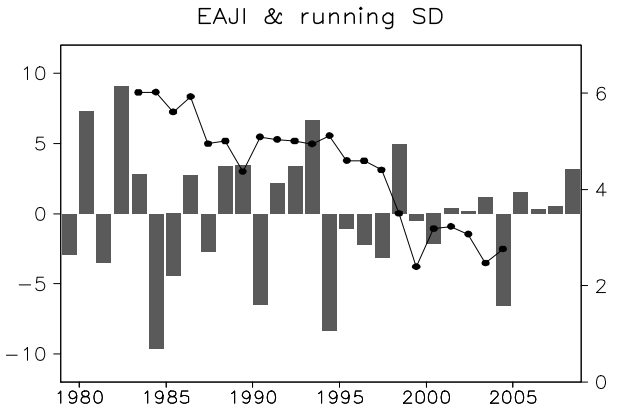

Fig. 3. Interannual variation of EAJI (labeled at the left) and 9-year, running window, standard deviation of the index (labeled at the right).

but there are only three years (1994, 1998 and 2004) during the latter period. One standard deviation of the EAJI is 5.21 during the former period and 3.28 during the latter period. This difference in the EAJI amplitude between the two periods is significant at the 95% confidence level according to the F-test. In the present study, following Kwon et al. (2005, 2007), the separating point was assigned as 1993–1994, to facilitate comparisons with previous results.

Figure 4 shows the zonal winds at 200 hPa during the two periods and the differences in the winds between the periods. Consistent with the result of Kwon et al. (2007), the zonal winds decrease significantly over North China and Northwest China (Fig. 4c). Such a decadal change makes the EAJ spatial structure different between the two periods: the jet stream becomes gradually weaker eastward over North China in the former period (Fig. 4a), but weakens more sharply over North China and increases slightly over Japan during the latter period (Fig. 4b). Over the regions defining the EAJI, i.e., (30°–50°N, 120°–150°E), no clear decadal change in the zonal winds is observed (Fig. 4c). In addition to this change in zonal wind, there is a significant northerly anomaly over Northeast Asia, which is consistent with the result of Kwon et al. (2007).

3. Changes in the dominant modes of EAJ variability since the mid-1990s

The saddle shape of the interannual standard deviation in the zonal wind over East Asia, i.e., the relatively stronger variability around 35°N and 45°N and the weaker variability around 40°N, is in agreement with the fact that the meridional displacement is a dominant feature of EAJ variability. Lin and Lu (2005) performed an EOF analysis on 200-hPa zonal

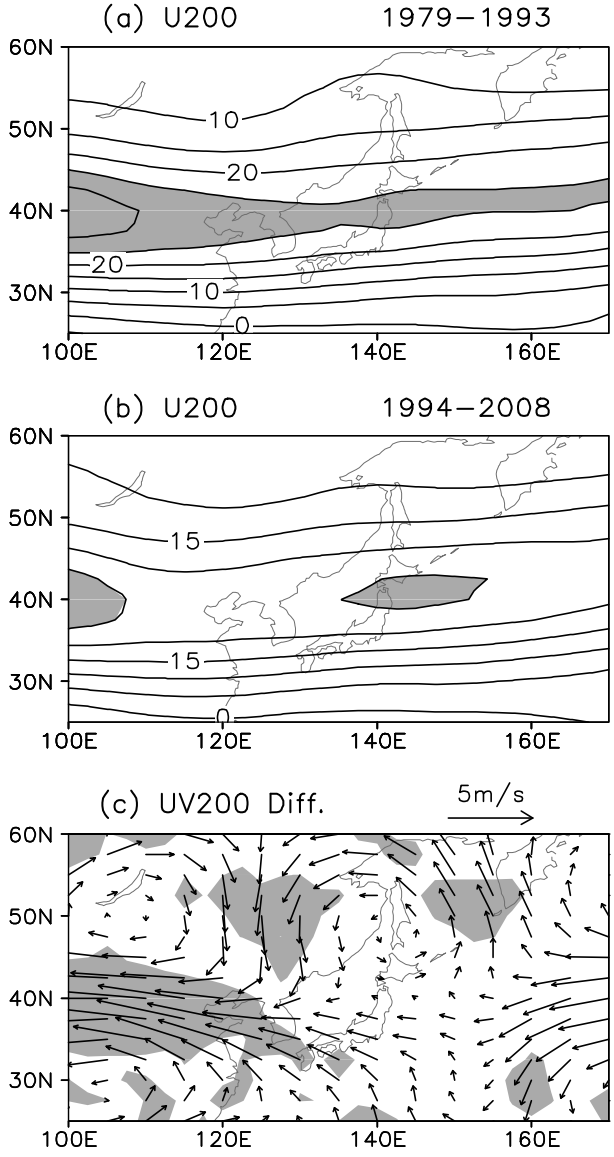

Fig. 4. JJA-mean 200-hPa zonal wind averaged over (a) 1979–1993 and (b) 1994–2008, and the difference in horizontal winds between these two periods (c). The contour interval is 5 m s^{-1}. Shading in (a) and (b) indicates the regions where the values are >25 m s^{-1}, and shading in (c) indicates the difference in either zonal or meridional wind significant at the 95% confidence level according to the Lepage test.

winds over the domain of 25°–55°N, 120°–150°E, using the NCEP/NCAR reanalysis data from 1979 to 2002. The first leading mode in their result is characterized by alternate signs south and north of the jet axis and by a zero contour line running roughly along the jet axis. Because this leading mode explains about half of the total variance, its spatial distribution may have contributed greatly to the saddle shape of the standard deviation of the zonal wind.

We repeated the EOF analysis on 200-hPa zonal winds over the same domain used by Lin and Lu (2005), but we used an extended period (1979–2008 in this study vs. 1979–2002 in the aforementioned one); the results are shown in Fig. 5. The zero contour line in the first mode (Fig. 5a) appears over almost the same location as the EAJ axis (Fig. 1a), and alternate signs appear south and north of the axis. Both the positive and negative anomalies, as well as the zero contour line, are zonally oriented but with a slight southwest–northeast tilt, consistent with the orientation of the jet stream over this region. Thus, the first mode represents the meridional displacement of the EAJ axis. Actually, the PC-1 is highly correlated with the EAJI, with the correlation coefficient between them being 0.945, which is significant at the 99% confidence level. The second mode exhibits maximum positive values along the EAJ axis (Fig. 5b), and thus represents the variability in the EAJ intensity. These results are consistent with those of Lin and Lu (2005).

Figure 6 shows the results of the EOF analysis for the former period. The EOF spatial patterns for this period (Figs. 6a and 6b) are quite similar to those for the whole period (Figs. 5a and 5b). A careful observation, however, indicates that the EOF spatial patterns for the former period are shifted southward in comparison to those for the whole period. At 120°E, for instance, the zero contour line of EOF-1 shifts southwards from ∼40°N for the whole period (Fig. 5a) to ∼38°N for the former period (Fig. 6a). This shift of the zero contour line is consistent with the fact that the EAJ axis is located slightly southward during 1979–1993 in comparison with the axis during 1979–2008 (Figs. 1a and 4a). The zero contour line of EOF-1 appears over almost the same location as the EAJ axis does. Therefore, the first mode also represents the meridional displacement of EAJ during the former period.

The EOF-1 during 1994–2008 (Fig. 7a), however, exhibits a pattern quite different from that of the EOF-1 during 1979–1993 or during 1979–2008. The zero line of the EOF-1 during 1994–2008 is located significantly northward in comparison with that of the EOF-1 during 1979–1993, while the jet axis during the latter period shifts northward only slightly in comparison with that during the former period. During 1994–2008, therefore, the EOF-1 confuses the meridional location and intensity of the EAJ, and the meridional displacement of the EAJ does not represent well the first mode. This result agrees with the fact that the EAJI variability is weakened significantly during the latter period.

Furthermore, both the positive and negative cells

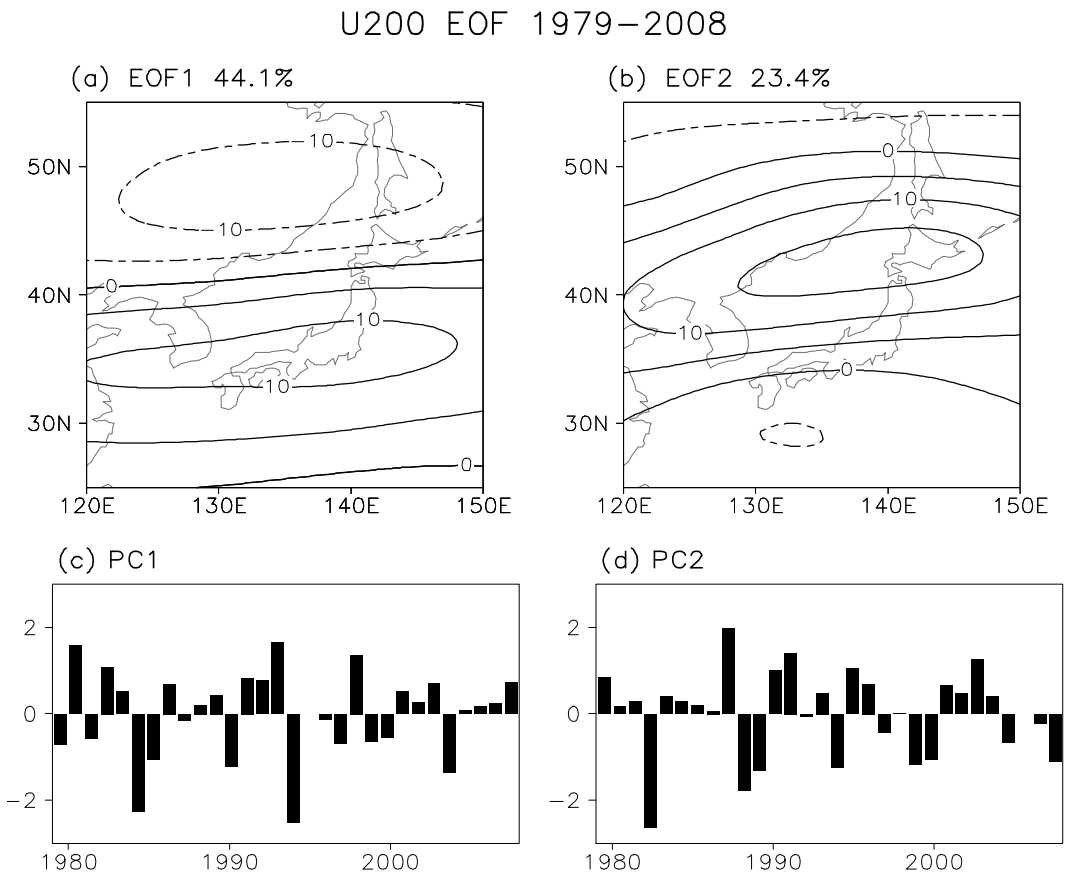

Fig. 5. Spatial distribution of the first and second leading EOF modes (a and b), and their principal components (c and d), for the period 1979–2008. The domain for the EOF analysis is the same as the shown, i.e., 25°–55°N, 120°–150°E.

of the first mode exhibit a clear southwest–northeast tilt during the former period (Fig. 6a), but they are zonally oriented during the latter period (Fig. 7a). On the other hand, the EOF-2 during the latter period (Fig. 7b) is also zonally oriented and even slightly tilted northwest–southeast, which is significantly inconsistent with the EOF-2 for both the former and the whole periods (Figs. 5b and 6b). Therefore, it can be concluded that both leading modes exhibit distinct spatial patterns between the former and latter periods.

The year 1994 has an extreme value for the PC-1 during 1994–2008 (Fig. 7c). In fact, the summer of 1994 was characterized by extremely anomalous upper-tropospheric circulations over East Asia and the WNP (e.g., Park and Schubert, 1997). To investigate whether this special year induced the pattern change in the EOF-1 during 1994–2008, we repeated the EOF analysis, removing the year 1994 from the analysis period, i.e., using the data from 1995 to 2008. The result (not shown) indicates that removing the year 1994 does not appreciably change the EOF-1 pattern, suggesting that the differences in the EOF-1 between the former and latter periods are robust.

4. Energetics of the anomalous patterns associated with the EAJ variability

In this section, we investigate the physical mechanism for the weakening of the EAJ interannual variability and the changes in the dominant modes since the mid-1990s. The use of an identical index is appropriate for comparing the features between the former and latter periods, so we used the EAJI, which is defined by the difference between the 200-hPa zonal wind anomalies averaged over the two fixed regions. Figure 8 shows the horizontal wind anomalies at 200 hPa regressed onto the EAJI. Before the regression, the EAJI was normalized during the whole period, the former period, and the latter period. As expected given the definition of the EAJI, westerly anomalies occurred south of 40°N and easterly anomalies occurred north of 40°N for all of the three periods, constructing a cyclonic circulation anomaly over the WNP and East Asia. These wind anomalies, however, exhibit distinct

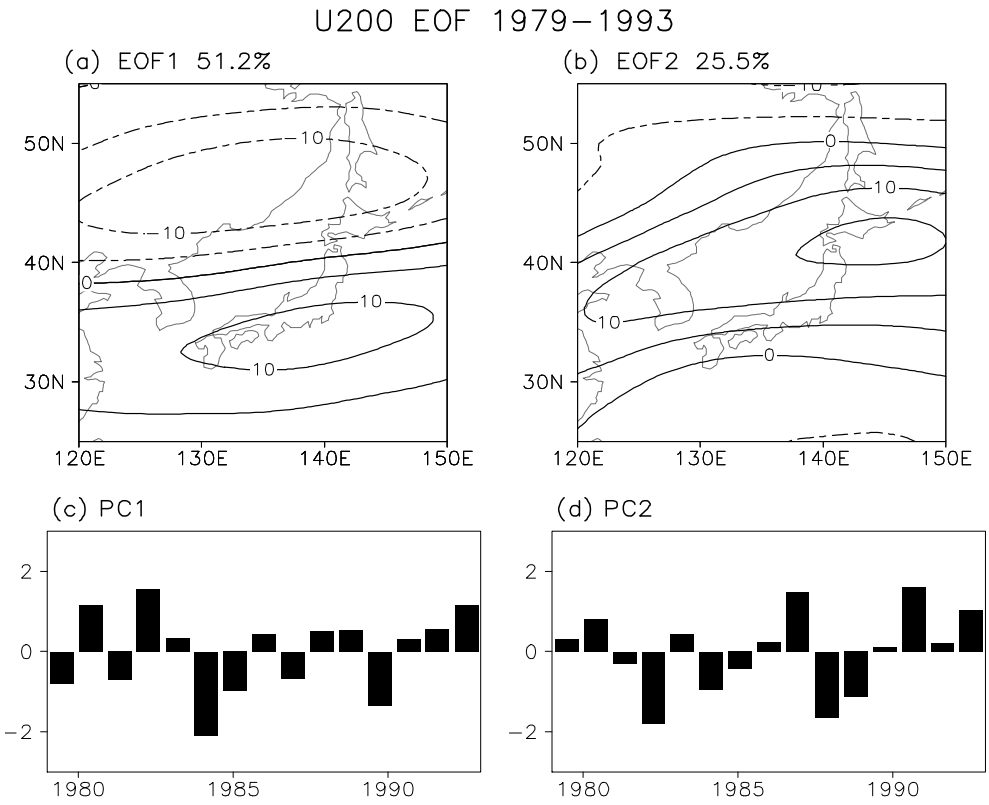

Fig. 6. Same as Fig. 5, but for 1979–1993.

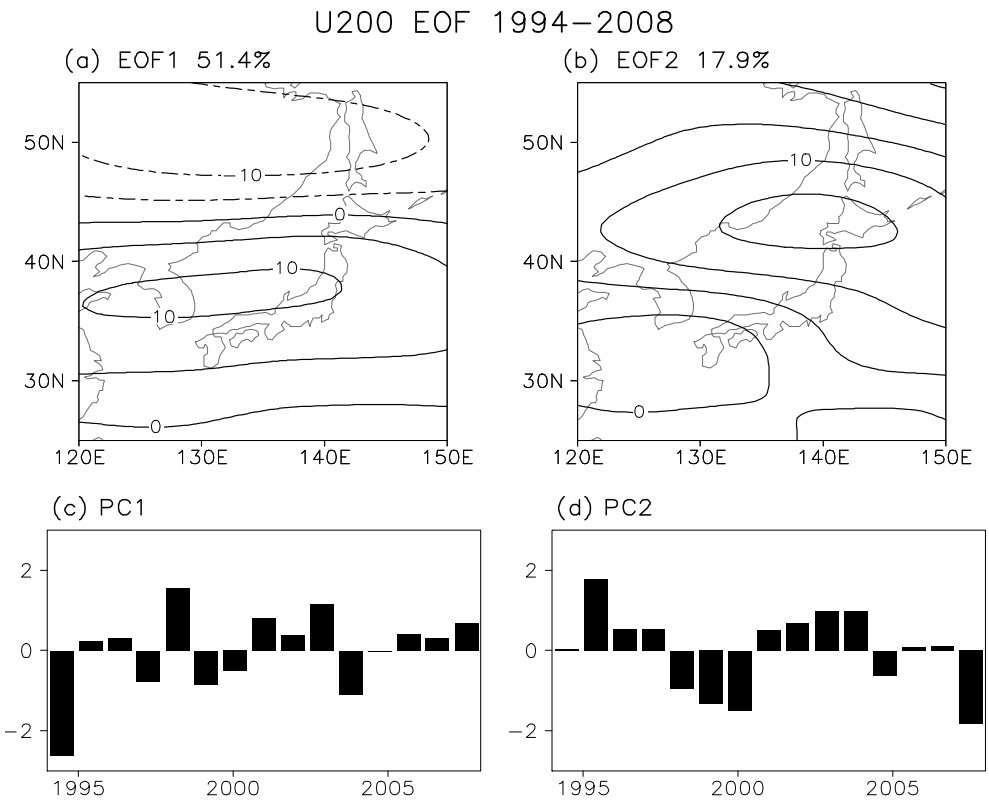

Fig. 7. Same as Fig. 5, but for 1994–2008.

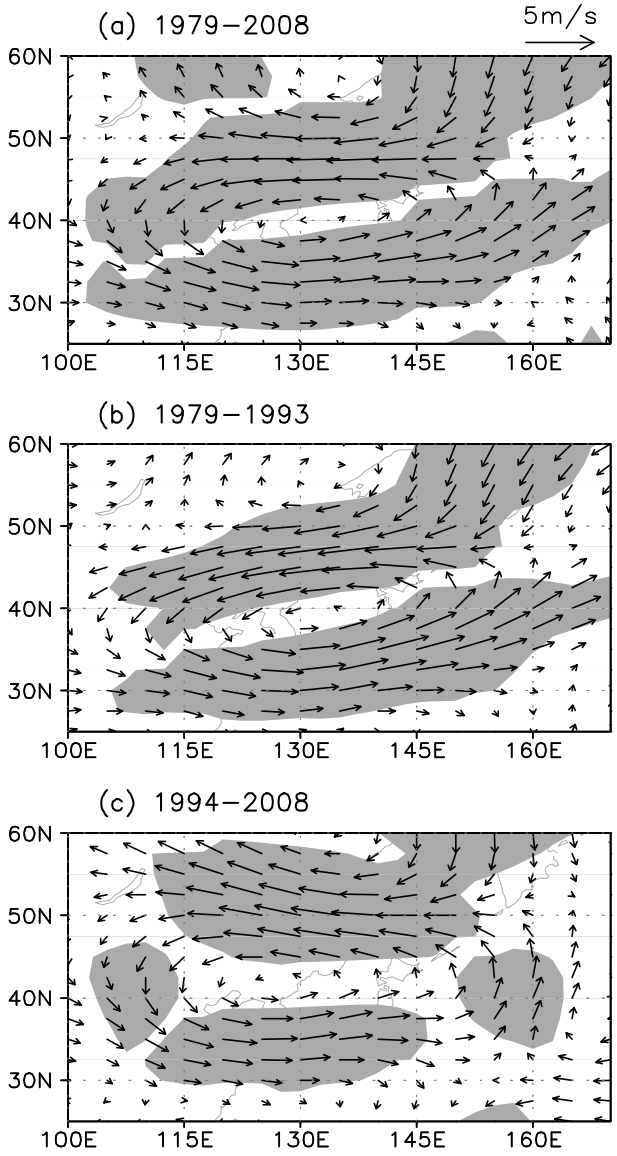

Fig. 8. 200-hPa wind anomalies regressed onto the standardized EAJI. (a) 1979–2008; (b) 1979–1993; (c) 1994–2008. Shading indicates the difference in either zonal or meridional wind significant at the 95% confidence level according to the t-test.

patterns between the former and latter periods. In the former period, the cyclonic anomaly is in a southwest–northeast direction (Fig. 8b), which is similar to the anomalous pattern for the whole period (Fig. 8a). In the latter period, however, the cyclonic anomaly is zonally oriented (Fig. 8c). This feature of the anomalous cyclone is in good agreement with the change in EOF-1 pattern shown in Figs. 5–7.

In the following analysis, the energetics of the anomalous patterns associated with the EAJI are summarized. Our approach was similar to that of Kosaka and Nakamura (2006, 2010), but with a major difference: the anomalies were regressed onto the EAJI in the present study, but they were regressed onto anomalous convection over the tropical WNP in Kosaka and Nakamura (2006, 2010). Three kinds of energy conversions or generations were discussed in Kosaka and Nakamura (2006, 2010): barotropic energy conversion, vertically integrated baroclinic conversion of available potential energy (APE), and vertically integrated APE generation due to anomalous diabatic heating. Our analyses, however, indicate that the vertical gradient in horizontal winds changes very little between the two periods in this study (not shown), although the horizontal winds themselves change significantly (shown partly by Fig. 4c). In addition, the intensity of precipitation variability, measured by the interannual standard deviation of summer precipitation, which is the main component of diabatic heating, basically does not weaken during the latter period (not shown). Thus, in this study, we focused only on the barotropic energy conversion.

The barotropic energy conversion of kinetic energy (KE) from the mean flow to the anomalies associated with the EAJI was calculated using the following formula:

$$\mathrm{CK} = \frac{v'^2 - u'^2}{2}\left(\frac{\partial \bar{u}}{\partial x} - \frac{\partial \bar{v}}{\partial y}\right) - u'v'\left(\frac{\partial \bar{u}}{\partial y} + \frac{\partial \bar{v}}{\partial x}\right), \quad (1)$$

where u and v represent the zonal and meridional velocities, respectively, overbars indicate the mean flows over a particular period, which could be 1979–2008, 1979–1993, or 1994–2008, and primes indicate the anomalies regressed onto the normalized EAJI during the particular period (shown in Fig. 8). Positive CK means the conversion of KE from the mean flow to the anomalies.

Figure 9 shows the local barotropic conversion CK during the three periods, respectively. Strong CK is concentrated in the region of the EAJI-associated cyclonic circulation anomaly (Fig. 8a). For the entire period, CK is positive at the western extent of the cyclonic anomaly, and tends to be negative at the eastern extent (Fig. 9a). Thus, the barotropic conversion acts to maintain the EAJI-associated cyclonic anomaly upstream of the EAJ and to dampen the anomaly downstream. The averages of CK over the WNP–EA and the northern hemisphere are 0.211 and 0.031, respectively (Table 1). These positive averages indicate that the anomalies associated with the EAJI obtain KE from the mean flow. Table 1 also shows that CK can replenish KE in 8.57 days when averaging over the WNP–EA and in 12.46 days when averaging over the northern hemisphere. These short time scales indicate that the conversion from the mean flow can effectively maintain the anomalies associated with EAJ variabil-

Table 1. Barotropic conversion CK averaged over the domain of the WNP and East Asia (25°–60°N, 100°–170°E), and over the entire northern hemisphere. Units: 10^{-5} m^2 s^{-3}. Shown in parentheses is the time scale (d) with which horizontally integrated KE could be replenished through barotropic conversion CK, which is calculated as the ratio of KE to CK.

Ave. domain	Period		
	1979–2008	1979–1993	1994–2008
25°–60°N, 100°–170°E	0.211 (8.57 d)	0.505 (4.89 d)	−0.199 (−8.09 d)
0°–90°N, 0°–360°E	0.031 (12.46 d)	0.111 (6.16 d)	−0.020 (−31.84 d)

ity.

It should be noted that the EAJI-regressed anomalies are "idealized eddies" in this study; that is, they are summer mean anomalies and thus do not change with time in a particular summer. This differs from previous studies (e.g., Hoskins et al., 1983; Simmons et al., 1983), in which eddies vary with time. No evolution implies no time scales for the replenishment of KE or for the growth of eddies. However, the objective of this study is to evaluate whether a particular anomalous pattern can effectively obtain energy from the basic flow. Thus, a strong positive value of CK or a short time scale suggests that one particular pattern of anomalies can be effectively maintained and thus may appear as a dominant mode.

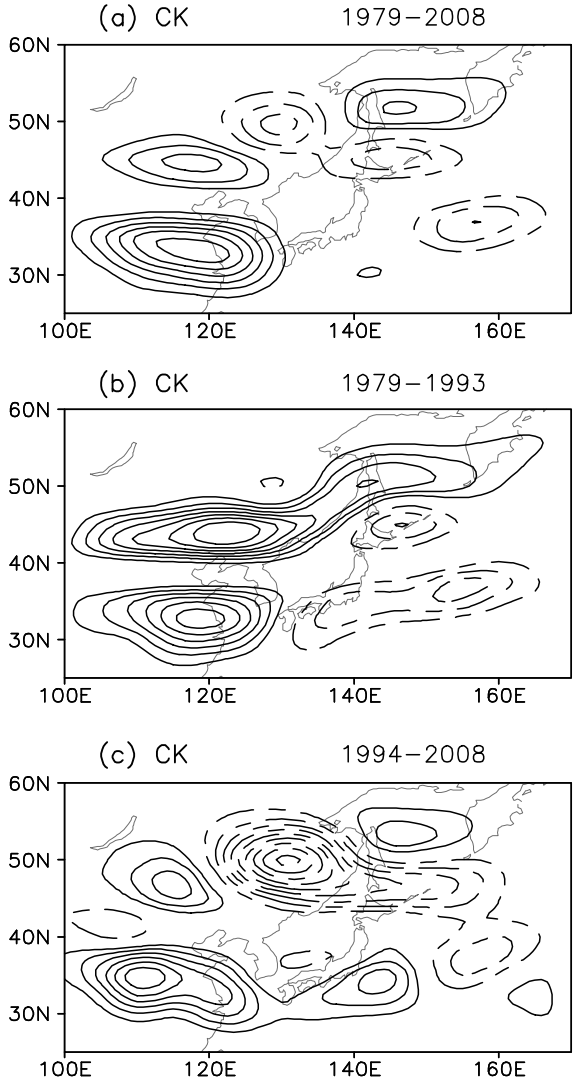

Fig. 9. Local barotropic conversion CK at 200 hPa. (a) 1979–2008; (b) 1979–1993; (c) 1994–2008. The contour interval is 1.0×10^{-5} m^2 s^{-2}.

The barotropic energy conversion CK exhibits a great difference between the former and latter periods (Figs. 9b and 9c), although the spatial distributions of CK during these two periods are similar to the result for the entire period (Fig. 9a). Positive CK over the western extent is much stronger during the former period than it is in the latter period, while negative CK over the eastern extent, at the point of area averaging, does not change much between the two periods. Therefore, the averages of CK over the WNP–EA and the northern hemisphere are strongly positive during the former period, but they become negative during the latter period (Table 1). In addition, the time scale during the former period is 4.89 days over the WNP–EA and is 6.16 days over the northern hemisphere, which are much shorter than that for the entire period. However, the time scale during the latter period is negative, which suggests that the anomalies provide energy to the basic flow. Consequently, the barotropic energy conversion can efficiently maintain the anomalies associated with the EAJ variability during the former period, but it dampens the anomalies during the latter period. Thus, it can be concluded that the remarkable change in the barotropic energy conversion has led to the weakening of EAJI variability and a change in the leading mode since the mid-1990s.

A question naturally arises: Why has the barotropic energy conversion experienced this weakening since the mid-1990s? The formula for CK indicates that CK is the product of the EAJI-regressed anomalies and horizontal gradients of the basic flow. Therefore, a change in CK can be categorized into the following three components:

The CK change induced by an anomaly change only:

$$\frac{1}{2}\left[\left(v'^2-u'^2\right)_{\rm L}-\left(v'^2-u'^2\right)_{\rm F}\right]\left(\frac{\partial\bar{u}}{\partial x}-\frac{\partial\bar{v}}{\partial y}\right)_{\rm F}- \left[\left(u'v'\right)_{\rm L}-\left(u'v'\right)_{\rm F}\right]\left(\frac{\partial\bar{u}}{\partial y}+\frac{\partial\bar{v}}{\partial x}\right)_{\rm F}. \quad (2)$$

The CK change induced by a basic flow change only:

$$\frac{1}{2}\left(v'^2-u'^2\right)_{\rm F}\left[\left(\frac{\partial\bar{u}}{\partial x}-\frac{\partial\bar{v}}{\partial y}\right)_{\rm L}-\left(\frac{\partial\bar{u}}{\partial x}-\frac{\partial\bar{v}}{\partial y}\right)_{\rm F}\right]- \left(u'v'\right)_{\rm F}\left[\left(\frac{\partial\bar{u}}{\partial y}+\frac{\partial\bar{v}}{\partial x}\right)_{\rm L}-\left(\frac{\partial\bar{u}}{\partial y}+\frac{\partial\bar{v}}{\partial x}\right)_{\rm F}\right]. \quad (3)$$

The residual:

$$\frac{1}{2}\left[\left(v'^2-u'^2\right)_{\rm L}-\left(v'^2-u'^2\right)_{\rm F}\right]\left[\left(\frac{\partial\bar{u}}{\partial x}-\frac{\partial\bar{v}}{\partial y}\right)_{\rm L}- \left(\frac{\partial\bar{u}}{\partial x}-\frac{\partial\bar{v}}{\partial y}\right)_{\rm F}\right]-\left[\left(u'v'\right)_{\rm L}-\left(u'v'\right)_{\rm F}\right]\times \left[\left(\frac{\partial\bar{u}}{\partial y}+\frac{\partial\bar{v}}{\partial x}\right)_{\rm L}-\left(\frac{\partial\bar{u}}{\partial y}+\frac{\partial\bar{v}}{\partial x}\right)_{\rm F}\right]. \quad (4)$$

The subscripts F and L indicate that the values in parenthesis are for the former and latter periods, respectively.

Table 2 shows that these three components of CK change from the former period to the latter period. The decrease in CK induced by the anomaly change is the largest, both for the averages over the WNP–EA domain and over the entire northern hemisphere. This decrease is about three to five times the size of the CK decrease induced by basic flow change. The third component, i.e., the residual, is weakly positive. Thus, the change in the EAJI-associated anomalies is a major reason for the CK decrease from the former period to the latter period, and the change in the mean flow also modestly contributes to the CK decrease.

This result, however, does not suggest that the change in the mean flow only plays a modest role in weakening the EAJI variability and changing the first mode of zonal wind. The above three categories are mathematically made, but in reality the change in the anomalies may be strongly dependent on the change in the mean flow. Thus, the result of the present category analysis indicates that the change in the EAJI-associated anomalies, which might be affected by the change in the mean flow, contributes greatly to the CK decrease from the former period to the latter period.

The change in the orientation of the EAJI-associated cyclonic anomaly is a crucial reason, among others, for the weakening of barotropic energy conversion. The anomalous cyclone is in a southwest–northeast direction in the former period (Fig. 8b), as well as for the entire period (Fig. 8a), but is zonally oriented in the latter period (Fig. 8c). It can be inferred from Fig. 8 that, at the western extent of the anomalous cyclone, $-u'v'$ is negative north of the EAJ axis and positive south of the EAJ axis, and thus the second term of CK, which is dominated by $-u'v'(\partial\bar{u}/\partial y)$ because $(\partial\bar{u}/\partial y)\gg(\partial\bar{v}/\partial x)$, is positive. Our analysis (not shown) indicates that this mechanism is mainly responsible for the positive CK at the western extent of the cyclonic circulation anomaly (Fig. 9). The quantity $-u'v'$ is closely associated with the orientation of the cyclonic anomaly, having smaller values and being over smaller areas for a zonally oriented anomaly pattern relative to a southwest–northeast tilted pattern. Therefore, CK is more strongly positive at the western extent of the cyclonic anomaly for the former period than it is for the latter period, which is in agreement with the results shown in Fig. 9. At the eastern extent of the anomalous cyclone, the positive and negative values of $-u'v'$ do not match well with the northern and southern areas of the EAJ axis, and thus $-u'v'(\partial\bar{u}/\partial y)$ does not exhibit a well-organized spatial distribution, unlike its western counterpart.

5. Conclusions

In this study, we found that interannual variability in the summer EAJ has significantly weakened since the mid-1990s. The interannual standard deviation of the upper-tropospheric zonal winds decreased over the WNP south of Japan and Northeast Asia,

Table 2. Changes in CK from the period 1979–1993 to the period 1994–2008, induced by the anomaly change only, by basic flow change only, and the residual. See the text for more details. Units: 10^{-5} m^2 s^{-3}.

Changing reason	Ave. domain	
	25°–60°N, 100°–170°E	0°–90°N, 0°–360°
Anomaly change	−0.625	−0.119
Basic flow change	−0.219	−0.023
Residual	0.139	0.012

and the standard deviation of the EAJI dropped from 5.21 during 1979–1993 to 3.28 during 1994–2008. This weakening in EAJ variability was concurrent with the changes in spatial patterns of the standard deviations of zonal winds. During 1979–1993, the spatial pattern of the standard deviation of 200-hPa zonal winds resembled a saddle shape: stronger interannual variability appeared north and south of the EAJ axis, and weaker variability occurred along the axis. The saddle shape, however, does not appear during 1994–2008. The saddle shape of interannual standard deviation in zonal winds is in agreement with the fact that the meridional displacement is a dominant feature of EAJ variability (Lin and Lu, 2005). Therefore, the leading mode represents the meridional displacement of EAJ with the saddle-shaped pattern of standard deviation for the former period, which is consistent with a previous study (Lin and Lu, 2005) but confuses the meridional location and intensity of the EAJ without a saddle-shaped pattern during the latter period.

The energetics of the anomalous patterns associated with the EAJI are examined to explain physically the possible reason for these changes in the EAJ variability and in the dominant modes. The results indicate that the change in the barotropic energy conversion CK between basic flows and anomalies led to a weakening of the EAJI variability and a change in the leading dominant mode since the mid-1990s. The averages of CK over either the WNP–EA or the northern hemisphere were strongly positive during the former period but negative during the latter period. Consequently, the barotropic energy conversion efficiently maintained the anomalies associated with the EAJ variability during the former period but acted to dampen the anomalies during the latter period.

Furthermore, the result of this study suggests that the change in the EAJI-associated anomalies, which might be affected by the mean flow change, contributes greatly to the CK change between the two periods and that the mean flow change itself also contributes modestly. Although this result cannot effectively distinguish the roles of the changes in the anomalies and mean flows because in reality the change in the anomalies may be strongly dependent on the mean flow change, it can be inferred that some particular anomalous patterns may be more efficiently maintained by the mean flow than other patterns can be. We found that both the circulation anomaly associated with the first leading mode and the EAJI exhibited distinct patterns between the former and latter periods. These anomalies exhibited a southwest–northeast tilt during the former period but are zonally oriented during the latter period. This change in the orientation of the circulation anomalies, indicated by an analysis of energy conversion, has been a crucial reason for the weakening of barotropic energy conversion since the mid-1990s.

Acknowledgements. This study was supported by the National Natural Science Foundation of China (Grant Nos. 40810059005 and 40725016). The authors thank the two anonymous reviewers for their helpful comments.

REFERENCES

Bueh, C., N. Shi, L. Ji, J. Wei, and S. Tao, 2008: Features of the EAP events on the medium-range evolution process and the mid- and high-latitude Rossby wave activities. *Chinese Science Bulletin*, **53**, 610–623.

Choi, K.-S., D.-W. Kim, and H.-R. Byun, 2009: Possible impact of spring sea ice anomaly in the North Pacific on the Korean summer drought. *Asia-Pacific J. Atmos. Sci.*, **45**, 331–346.

Enomoto, T., B. J. Hoskins, and Y. Matsuda, 2003: The formation mechanism of the Bonin high in August. *Quart. J. Roy. Meteor. Soc.*, **129**, 157–178.

Fu, J., S. Li, and D. Luo, 2009: Impact of global SST on decadal shift of East Asian summer climate. *Adv. Atmos. Sci.*, **26**, 192–201, doi: 10.1007/s00376-009-0192-z.

Gong, D., and C.-H. Ho, 2002: Shift in the summer rainfall over the Yangtze River valley in the late 1970s. *Geophys. Res. Lett.*, **29**, 1436, doi: 0.1029/2001GL014523.

Gu, W., C. Li, X. Wang, W. Zhou, and W. Li, 2009: Linkage between mei-yu precipitation and North Atlantic SST on the decadal timescale. *Adv. Atmos. Sci.*, **26**, 101–108, doi: 10.1007/s00376-009-0101-5.

Hoskins, B. J., I. N. James, and G. H. White, 1983: The shape, propagation and mean-flow interaction of large-scale weather systems. *J. Atmos. Sci.*, **40**, 1595–1612.

Hsu, H. H., and S. M. Lin, 2007: Asymmetry of the tripole rainfall pattern during the East Asian summer. *J. Climate*, **20**, 4443–4458.

Huang, R., and F. Sun, 1992: Impacts of the tropical western Pacific on the East Asian summer monsoon. *J. Meteor. Soc. Japan*, **70**, 243–256.

Huang, R., Y. Xu, and L. Zhou, 1999: The interdecadal variation of summer precipitation in China and the drought trend in North China. *Plateau Meteorology*, **18**, 465–476. (in Chinese)

Kim, C.-J., W. Qian, H.-S. Kang, and D.-K. Lee, 2010: Interdecadal variability of East Asian summer monsoon precipitation over 220 years (1777–1997). *Adv. Atmos. Sci.*, **27**, 253–264, doi: 10.1007/s00376-009-8079-6.

Kosaka, Y., and H. Nakamura, 2006: Structure and dynamics of the summertime Pacific-Japan teleconnection pattern. *Quart. J. Roy. Meteor. Soc.*, **132**, 2009–2030.

Kosaka, Y., and H. Nakamura, 2010: Mechanisms of meridional teleconnection observed between a sum-

mer monsoon system and a subtropical anticyclone. part I: the Pacific-Japan pattern. *J. Climate*, **23**, 5085–5108.

Kwon, M., J.-G. Jhun, B. Wang, S.-I. An, and J.-S. Kug, 2005: Decadal change in relationship between east Asian and WNP summer monsoons. *Geophys. Res. Lett.*, **32**, L16709, doi: 10.1029/2005GL023026.

Kwon, M., J.-G. Jhun, and K.-J. Ha, 2007: Decadal change in East Asian summer monsoon circulation in the mid-1990s. *Geophys. Res. Lett.*, **34**, L21706, doi: 10.1029/2007GL031977.

Kurihara, K., and T. Tsuyuki, 1987: Development of the barotropic high around Japan and its association with Rossby wave-like propagations over the North Pacific: Analysis of August 1984. *J. Meteor. Soc. Japan*, **65**, 237–246.

Lau, K.-M, K.-M. Kim, and S. Yang, 2000: Dynamical and boundary forcing characteristics of regional components of the Asian summer monsoon. *J. Climate*, **13**, 2461–2482.

Li, C., J. He, and J. Zhu, 2004: A review of decadal/interdecadal climate variation studies in China. *Adv. Atmos. Sci.*, **21**, 425–436.

Li, S., and G. T. Bates, 2007: Influence of the Atlantic multidecadal oscillation on the winter climate of East China. *Adv. Atmos. Sci.*, **24**, 126–135, doi: 10.1007/s00376-007-0126-6.

Lin, Z., and R. Lu, 2005: Interannual meridional displacement of the East Asian upper-tropospheric jet stream in summer. *Adv. Atmos. Sci.*, **22**, 199–211.

Lin, Z., and R. Lu, 2009: The ENSO's effect on the eastern China rainfall in the following early summer. *Adv. Atmos. Sci.*, **26**, 333–342, doi: 10.1007/s00376-009-0333-4.

Lin, Z., R. Lu, and W. Zhou, 2010: Change in early-summer meridional teleconnection over the western North Pacific and East Asia around the late 1970s. *Int. J. Climatol.*, **30**, 2195–2204.

Lu, R., 2004: Associations among the components of the East Asian summer monsoon system in the meridional direction. *J. Meteor. Soc. Japan*, **82**, 155–165.

Lu, R., and Z. Lin, 2009: Role of subtropical precipitation anomalies in maintaining the summertime meridional teleconnection over the western North Pacific and East Asia. *J. Climate*, **22**, 2058–2072.

Lu, R., and Y. Fu, 2010: Intensification of East Asian summer rainfall interannual variability in the twenty-first century simulated by 12 CMIP3 coupled models. *J. Climate*, **23**, 3316–3331.

Lu, R.-Y., J.-H. Oh, and B.-J. Kim, 2002: A teleconnection pattern in upper-level meridional wind over the North African and Eurasian continent in summer. *Tellus*, **54A**, 44–55.

Lu, R., B. Dong, and H. Ding, 2006: Impact of the Atlantic multidecadal oscillation on the Asian summer monsoon. *Geophys. Res. Lett.*, **33**, L24701, doi: 10.1029/2006GL027655.

Nitta, T., 1987: Convective activities in the tropical western Pacific and their impact on the Northern Hemisphere summer circulation. *J. Meteor. Soc. Japan*, **65**, 373–390.

Park, C.-K., and S. D. Schubert, 1997: On the nature of the 1994 East Asian summer drought. *J. Climate*, **10**, 1056–1070.

Sampe, T., and S.-P. Xie, 2010: Large-scale dynamics of the Meiyu-Baiu rain band: Environmental forcing by the westerly jet. *J. Climate*, **23**, 113–134.

Shi, N., C. Bueh, L. Ji, and P. Wang, 2009: The Impact of mid- and high-latitude Rossby wave activities on the medium-range evolution of the EAP pattern during the pre-rainy period of South China. *Acta Meteorologica Sinica*, **23**, 300–314.

Shi, S., and R. Lu, 2010: Teleconnection patterns along the Asian jet associated with different combinations of convection oscillations over the Indian continent and western North Pacific during summer. *Atmos. Oceanic Sci. Lett.*, **3**, 14–18.

Simmons, A. J., J. M. Wallace, and G. W. Branstator, 1983: Borotropic wave propagation and instability, and atmospheric teleconnection patterns. *J. Atmos. Sci.*, **40**, 1363–1392.

Wang, H., 2001: The weakening of the Asian monsoon circulation after the end of 1970's. *Adv. Atmos. Sci.*, **18**, 376–386.

Wang, B., R. Wu, and K.-M. Lau, 2001: Interannual variability of the Asian summer monsoon: Contrasts between the Indian and the western North Pacific-East Asian monsoons. *J. Climate*, **14**, 4073–4090.

Wu, B., K. Yang, and R. Zhang, 2009: Eurasian snow cover variability and its association with summer rainfall in China. *Adv. Atmos. Sci.*, **26**, 31–44, doi: 10.1007/s00376-009-0031-2.

Wu, R., Z. Wen, S. Yang, and Y. Li, 2010: An interdecadal change in southern China summer rainfall around 1992/93. *J. Climate*, **23**, 2389–2403.

Yim, S.-Y., J.-G. Jhun, and S.-W. Yeh, 2008a: Decadal change in the relationship between east Asian-western North Pacific summer monsoons and ENSO in the mid-1990s. *Geophys. Res. Lett.*, **35**, L20711, doi: 10.1029/2008GL035751.

Yim, S.-Y., S.-W. Yeh, R. Wu, and J.-G. Jhun, 2008b: The influence of ENSO on decadal variations in the relationship between the East Asian and western North Pacific summer monsoons. *J. Climate*, **21**, 3165–3179.

Yu, R., and T. Zhou, 2007: Seasonality and three-dimensional structure of interdecadal change in the East Asian monsoon. *J. Climate*, **20**, 5344–5355.

Yun, K.-S., K.-J. Ha, B. Wang, and R. Ding, 2010: Decadal cooling in the Indian summer monsoon after 1997/1998 El Niño and its impact on the East Asian summer monsoon. *Geophys. Res. Lett.*, **37**, L01805, doi: 10.1029/2009GL041539.

Zhang, Y., X. Kuang, W. Guo, and T. Zhou, 2006: Seasonal evolution of the upper-tropospheric westerly jet core over East Asia. *Geophys. Res. Lett.*, **33,** L11708, doi: 10.1029/2006GL026377.

Zhou, T., and Coauthors, 2009: Why the western Pacific

subtropical high has extended westward since the late 1970s. *J. Climate*, **22**, 2199–2215.

Zhu, J., and S. Wang, 2001: 80a-oscillation of summer rainfall over the east part of China and East-Asian summer monsoon. *Adv. Atmos. Sci.*, **18**, 1043–1051.

Zhu, Y., and X. Yang, 2003: Relationships between Pacific Decadal Oscillation (PDO) and climate variabilities in China. *Acta Meteorologica Sinica*, **61**, 641–654. (in Chinese)

Zhu, Y., H. Wang, W. Zhou, and J. Ma, 2010: Recent changes in the summer precipitation pattern in East China and the background circulation. *Climate Dyn.*, **36**, 1463–1473.